

HSAB principle and nickel(II) ion reactivity towards 1-methylhydantoin

Mariola Puszyńska-Tuszkano^a, Marek Daszkiewicz^b, Gabriela Maciejewska^a, Zbigniew Staszak^c,
Joanna Wietrzyk^d, Beata Filip^d, Maria Cieślak-Golonka^{a,*}

^a Faculty of Chemistry, Wrocław University of Technology, Wybrzeże Wyspiańskiego 27, 50-370 Wrocław, Poland

^b Institute of Low Temperature and Structure Research, Polish Academy of Sciences, Okólna 2, P.O. Box 1410, 50-950 Wrocław, Poland

^c Institute of Informatics, Wrocław University of Technology, Wybrzeże Wyspiańskiego 27, 50-370 Wrocław, Poland

^d Ludwik Hierszfeld Institute of Immunology and Experimental Therapy, Polish Academy of Science, Rudolf Weigl Str. 12, 53-114 Wrocław, Poland

ARTICLE INFO

Article history:

Received 31 January 2011

Accepted 6 May 2011

Available online 13 May 2011

Keywords:

Nickel ion

Hydantoin derivative

Structure

Spectroscopic properties

HSAB theory

Spectrochemical series

ABSTRACT

1-Methylhydantoin and its novel nickel(II) complex $[\text{Ni}(\text{H}_2\text{O})_4(1\text{-mhyd})_2]$ were prepared and identified, by elemental analysis, single crystal X-ray determination and MS methods. In addition, the complex was characterized by spectroscopic (IR, UV–Vis), magnetic and thermal techniques. The ligand reveals an interesting supramolecular architecture with both classical and non-conventional extended HB bonding networks. All rings and chains formed due to this HB bonding are embedded into the undulated pattern. A single crystal X-ray diffraction analysis of the complex shows that the nickel ion is coordinated by deprotonated hydantoin and water ligands in a N_2O_4 tetragonal arrangement. In the $[\text{Ni}(\text{H}_2\text{O})_4(1\text{-mhyd})_2]$ structure both inter and intramolecular hydrogen bonds are created with the participation of water molecules.

The ESI-MS method confirmed mono-nuclearity of the complex while electronic spectroscopy proved the tetragonal and pseudo-octahedral geometries around the metal ion in the solid state and solution, respectively. By application of the “average environment rule”, 10Dq parameters were obtained for the hypothetical, hexa-coordinate $[\text{Ni}(1\text{-mhyd})_6]$ approximation or rather more realistic $[\text{Ni}(1\text{-mhyd})_3]$ chelate. Based on this the mhyd ligand was ranked in the spectrochemical series close to ammonia. The general consideration of the structure of the hydantoin complexes as a function of the metal ion hardness within the framework of the HSAB theory has been provided. Both the ligand and the complex were found to be non-toxic agents against breast (MCF-7), lung carcinoma epithelial (A549) and mouse fibroblasts (Balb/3T3) cancer cell lines.

© 2011 Elsevier Ltd. All rights reserved.

1. Introduction

1-Methylhydantoin (dioxy-creatinine, N-methylhydantoin, N-methylimidazolidine-2,4-dione) (Scheme 1) belongs to a large group of compounds generally called hydantoins. Studies on parent hydantoin and its various derivatives are of fundamental and practical importance due to their physiological action as anticonvulsant, antiepileptic, anti-inflammatory and anticancer drugs [1–4,7,8]. Recently, the potential application of compounds containing a hydantoin fragment for HIV-1 treatment has been also suggested [5,6]. In addition, 1-methylhydantoin-2-imide (creatinine) has been used as a skin cosmetic ingredient [9].

As complexation to a metal ion usually modifies the biological activity of a ligand [10], the coordination properties of various hydantoins including 1-mhyd, have been also studied [11–14]. However, to the best of our knowledge there are only four known metal complexes with 1-methylhydantoin: $\text{Na}[\text{Au}(1\text{-mhyd})_2] \cdot 4\text{H}_2\text{O}$, $[\text{Pt}_2(\text{NH}_3)_4(1\text{-mhyd})_2]_2(\text{NO}_3)_4 \cdot \text{H}_2\text{O}$, $[\text{Hg}(1\text{-mhyd})_2]_n$, and $\{\text{Ag}(1\text{-mhyd})\} \cdot 0.5\text{H}_2\text{O}\}_n$ [11–14]. In the gold(I) complex the metal ion coordinates two ligands deprotonated at N(3) (Scheme 1) [11]. In contrast, the crystal structure of other complexes with hydantoins exhibited rather complicated pattern of coordination modes through deprotonated N(3) of the ring to one metal ion and O(4) to the other [12,13]. (In addition, some further complications were found e.g. in the silver complexes due to argentophilic interactions) [14].

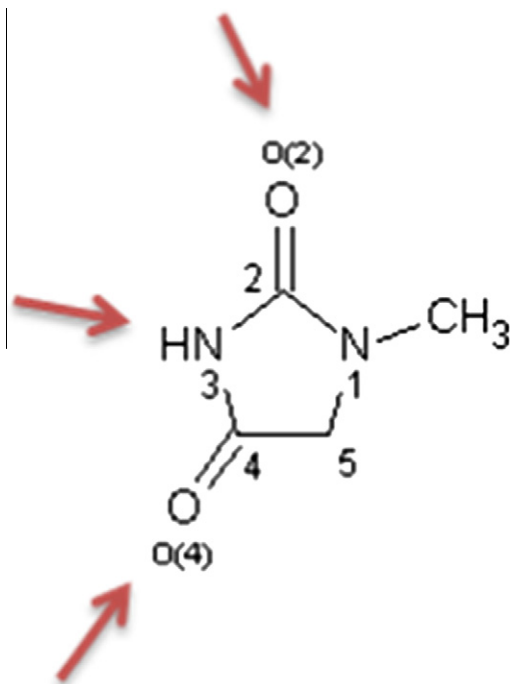
All central metal ions in the isolated 1-methylhydantoinate complexes belong to the soft Lewis acids group (HSAB) [15]. Thus, it would be of interest:

(a) to investigate, if the borderline and hard Lewis acids can interact with this ligand and if so, how are they bound;

- (b) to pursue a more general correlation of the structure of known metal complexes with other hydantoin derivatives with the hardness (or softness) of Lewis acids. This may shed more light on the understanding of the interaction of these ligands with metal ions.

* Corresponding author. Tel.: +48 71 320 22 80; fax: +48 71 320 43 60.

E-mail address: maria.golonka@pwr.wroc.pl (M. Cieślak-Golonka).



Scheme 1. Structure of 1-methylhydantoin (1-mhyd) and its potential binding sites.

- (c) to characterize the strength of 1-methylhydantoinate ligand through its ranking in the spectrochemical scale; and finally,
- (d) due to medical importance of the hydantoins to study cytotoxic activity of the ligand alone as well as its metal complexes.

In this work we have selected the nickel ion as the Lewis acid because it belongs to a large group of metal ions exhibiting a borderline hardness while at the same time being biologically interesting [16,17].

As a natural extension of the crystallographic study of the complex, the structure of the ligand has also been determined and reported herein.

2. Experimental

2.1. Crystallization of 1-methylhydantoin (**L**¹)

Crystals suitable for a single crystal X-ray diffraction determination were obtained by slow recrystallization of the compound (Aldrich Co.) from acetonitrile. *Anal. Calc.* for C₄H₆N₂O₂ (**L**¹) (*M_r* = 114.11 g/mol): C, 42.12; H, 5.26; N, 24.55. Found: C, 42.00; H, 4.82; N, 24.04%. Yield: 75%. Colour: white.

2.2. Preparation of [Ni(H₂O)₄(1-mhyd)₂] (**1**)

Blue crystals of (**1**) were prepared as follows: 0.1 mM (0.240 g) of NiCl₂·6H₂O dissolved in 10 cm³ of water was added to 0.2 mM (0.280 g) of 1-methylhydantoin dissolved also in 10 cm³ of water. Finally, to adjust pH value to ~8.0, 1 cm³ of 0.05 M KOH aqueous solution was added. The obtained bright blue solution was allowed to evaporate at room temperature to ca. 10 cm³ of volume. After 72 h, blue crystals of X-ray measurement quality were obtained. The product was filtered off and dried in vacuum. The crystals were stable at room temperature and soluble in methanol, DMSO and DMF. *Anal. Calc.* for C₈H₁₈NiN₄O₈ (*M_r* = 356.95 g/mol): C, 26.91;

H, 5.07; N, 15.70. Found: C, 27.18; H, 5.15; N, 15.91%. Yield: 21%. Magnetic moment: 2.77 BM.

2.3. Physicochemical studies

Elemental analyses were performed with a model Perkin–Elmer Analyzer 2400 (CHN) and AES-ICP 3410 emission spectrometer (Ni) using appropriate Aldrich standards. IR and FIR spectra of both the complex and the ligand were recorded as pellets or Nujol mulls using Perkin–Elmer FTIR 2000 (600–100 cm⁻¹) and Perkin–Elmer 1600 spectrophotometer in the range 4000–400 cm⁻¹.

The electronic spectra (5000–30 000 cm⁻¹) were measured on a Cary 500 Scan UV–Vis–NIR Spectrophotometer (Varian) in diffuse reflectance and absorption in methanol solution modes. In order to obtain accurate values of the band positions, the spectra were analyzed using variable digital filter method [18–24] with the following filter parameters: number determining the degree of resolution enhancement, $\alpha = 200.0$; the integer number determining the filter width, $N = 10$; the increment between points (step) = 100 cm⁻¹. For the d–d transition calculations of the crystal field the values of Dq (O_h) and Dq, Ds, Dt (D_{4h}) as well as Racah B parameters for both octahedral and tetragonal symmetries have been carried out. These calculations were based on the Tanabe–Sugano diagrams and Perumareddi matrices (without spin–orbit coupling parameter) for spin allowed transitions [25–27].

Thermogravimetric (TG) and differential thermal analyses (DTA) were carried out in nitrogen atmosphere, over 40–1000 °C range with a heating rate of 10° min⁻¹ using thermogravimetry TG-DTA system Setaram SETSYS 16/18. Calcined Al₂O₃ was used as the reference material.

Magnetic moments were measured using an MSB-MKI instrument (Sherwood Scientific Ltd.) at ambient temperature with Co[Hg(SCN)₄] as the standard.

Electrospray mass spectra (ESI-MS) were obtained in methanol solution as positive (ESI+) and negative (ESI-) ion mode on a Waters ESI-Q-TOF Premier XE. Additionally, Electron Ionisation mass spectra (EI) for the ligand were obtained on a Waters GCT Premier instrument.

2.4. X-ray structure determination

Diffraction data for (**L**¹) and (**1**) were collected on a Oxford Diffraction four-circle single crystal diffractometer equipped with a CCD detector using graphite-monochromated Mo K α radiation ($\lambda = 0.71073$ Å). The raw data were integrated with the CRYSDALS Data Reduction Program (version 1.172.32.6) and included the absorption and polarization effects. The intensities were corrected for Lorentz and polarization effects. Crystal structures were solved by the direct methods and refined by a full-matrix least-squares method using SHELXL-97 program [28]. All non-hydrogen atoms were refined with anisotropic displacement parameters. The H-atoms were located from the difference Fourier maps and refined assuming a ‘ride-on’ model.

2.5. Antiproliferative activity

The anti-proliferative tests were performed *in vitro* on human cancer cell lines MCF-7 (breast adenocarcinoma), A549 (non-small cell lung carcinoma) and mouse fibroblast cell line (Balb/3T3). Twenty-four hours before addition of the tested compounds, the cells were plated in 96-well plates (Sarstedt, Germany) at density of 10⁴ cells per well and cultured in the mixture medium. The breast cancer cells were cultured in Eagle medium supplemented with 2 mM glutamine (Sigma–Aldrich Chemie GmbH, Steinheim, Germany), amino acids and insulin (Sigma–Aldrich Chemie GmbH, Steinheim, Germany). The lung carcinoma cells were cultured in

the mixture of RPMI 1640 and Opti-MEM (1:1) medium (where RPMI and Opti-MEM are standard reagents used for cell culture [29]). In this case the RPMI 1640 was supplemented with 2 mM glutamine. The fibroblast cells were cultured in Dulbecco medium supplemented with 4 mM glutamine and glucose. All media were supplemented with 100 mg/cm³ streptomycin (Polfa, Tarchomin, Poland), 100 µg/cm³ penicillin (Polfa, Tarchomin, Poland), 5% (A549) or 10% (MCF-7, Balb/3T3) fetal bovine serum (Sigma–Aldrich Chemie GmbH, Steinheim, Germany). The cells were cultured at 37 °C in humid atmosphere saturated with 5% CO₂.

The *in vitro* cytotoxic effect of all compounds was examined after 96-h exposure of the cultured cells to varying concentrations of the tested compounds, using the SRB assay for adherent cells [29]. The results are presented as the IC50 value (inhibitory concentration 50%), i.e. the concentration (µg/cm³) of tested agent which inhibits proliferation of 50% of cancer cells population). A compound showing activity lower than 50% measured for 100 µg/cm³ was considered an inactive agent [29]. IC50 values were calculated separately for each experiment. Each compound was re-tested at every concentration in triplicate in a single experiment, which was repeated 3 times.

3. Results and discussion

The interaction of nickel(II) chloride with 1-methylhydantoin in aqueous solution resulted in precipitation of the mononuclear complex: *trans*-[Ni(H₂O)₄(mhyd)₂] (1). Its structure determination revealed tetragonally distorted coordination polyhedron around the metal ion involving two N(3) atoms, one from each 1-methylhydantoin anion and the O atoms of four water molecules.

3.1. Crystal structure of the 1-methylhydantoin (L¹)

The results of the X-ray analysis for 1-methylhydantoin are shown in Tables 1–3 and illustrated in Fig. 1.

Table 1

Crystal data and structure refinement parameters for 1-methylhydantoin (L¹) and [Ni(H₂O)₄(mhyd)₂] (1).

Compound	(L ¹)	(1)
Empirical formula	C ₄ H ₆ N ₂ O ₂	C ₈ H ₁₈ N ₄ NiO ₈
Formula weight	114.11	356.97
Temperature (K)	295(2)	295(2)
Wavelength (Å)	0.71073	0.71073
Crystal system, space group	Monoclinic, P2 ₁ /c	Monoclinic, P2 ₁ /c
<i>Unit cell dimensions</i>		
<i>a</i> (Å)	5.6010(10)	6.9349(5)
<i>b</i> (Å)	12.178(3)	12.1963(11)
<i>c</i> (Å)	8.090(2)	8.0162(8)
β (°)	105.64(2)	96.29(1)
Volume (Å ³)	531.4(2)	673.9(1)
<i>Z</i> , <i>D</i> _{calc} (g/cm ³)	4, 1.426	2, 1.759
Absorption coefficient (mm ⁻¹)	0.116	1.487
<i>F</i> (0 0 0)	240	372
Crystal size (mm)	0.37 × 0.35 × 0.35	0.32 × 0.28 × 0.23
θ Range for data collection (°)	3.35–27.48	3.34–27.48
Limiting indices	–7 ≤ <i>h</i> ≤ 7 –15 ≤ <i>k</i> ≤ 15 –10 ≤ <i>l</i> ≤ 10	–9 ≤ <i>h</i> ≤ 9 –15 ≤ <i>k</i> ≤ 15 –10 ≤ <i>l</i> ≤ 10
Reflections collected/unique	4850/1215 [<i>R</i> _{int} = 0.0755]	9589/1524 [<i>R</i> _{int} = 0.0512]
Completeness to θ	99.2%	99.1%
Absorption correction	None	Numerical
Maximum and minimum transmission		0.886 and 0.721
Refinement method	Full-matrix least-squares on <i>F</i> ²	Full-matrix least-squares on <i>F</i> ²
Data/restraints/parameters	1215/0/98	1524/0/98
Goodness-of-fit on <i>F</i> ²	0.963	1.01.1087
Final <i>R</i> indices [<i>I</i> > 2σ(<i>I</i>)]	<i>R</i> ₁ = 0.0403, <i>wR</i> ₂ = 0.1068	<i>R</i> ₁ = 0.0321, <i>wR</i> ₂ = 0.0897
<i>R</i> indices (all data)	<i>R</i> ₁ = 0.0583, <i>wR</i> ₂ = 0.1165	<i>R</i> ₁ = 0.0366, <i>wR</i> ₂ = 0.0923
Extinction coefficient	0.034(11)	None
Largest differences in peak and hole (e Å ⁻³)	0.181 and –0.160	0.387 and –0.512

Table 2

Selected bond lengths [Å] and angles [°] for 1-methylhydantoin (L¹) and [Ni(H₂O)₄(1-mhyd)₂] (1).

Bond lengths [Å]		Angles [°]	
(L¹)			
N(3)–H(3)	0.931(19)	N(3)–C(4)–O(4)	111.87(13)
N(1)–C(1)	1.444(2)	C(4)–N(3)–H(3)	126.4(10)
N(1)–C(2)	1.3323(18)	C(2)–N(3)–H(3)	121.6(10)
C(2)=O(2)	1.2278(18)	N(1)–C(2)–O(2)	127.47(13)
N(3)–C(2)	1.3915(18)	N(3)–C(2)–O(2)	124.60(13)
N(3)–C(4)	1.3595(19)	N(1)–C(2)–N(1)	107.91(13)
C(4)=O(4)	1.2110(18)	C(2)–N(1)–C(1)	123.51(14)
(1)			
Ni–OW1	2.0605(14)	N(3)#1–Ni–N(3)	180.00(9)
Ni–OW2	2.1239(14)	N(3)#1–Ni–OW1#1	89.82(6)
Ni–N(3)	2.1005(17)	N(3)#1–Ni–OW1	90.18(6)
Ni–OW1#1	2.0605(14)	N(3)–Ni–OW1#1	90.18(6)
Ni–OW2#2	2.1239(14)	N(3)–Ni–OW1	89.82(6)
Ni–N(3)#3	2.1005(17)	OW2#1–Ni–OW2	180.00
		OW1#1–Ni–OW2#1	89.62(6)
		OW1–Ni–OW2#1	90.38(6)
		N(3)#1–Ni–OW2#1	91.00(6)
		N(3)–Ni–OW2#1	89.00(6)
		OW1#1–Ni–OW2	90.38(6)
		OW1–Ni–OW2	89.62(6)
		N(3)#1–Ni–OW2	89.00(6)
		N(3)–Ni–OW2	91.00(6)
		OW1#1–Ni–OW1	180.00(8)

Symmetry codes: #1 –*x*, –*y* + 1, –*z* + 1.

The distances and angles around the heterocyclic hydantoin ring are in good agreement and compare well with those found in the parent hydantoin and its various derivatives like e.g. 5,5-dimethyl(diphenyl) hydantoins [30–33]. The hydantoin ring in 1-mhyd can be classified as essentially planar. The C(2)=O(2) bond length is slightly longer than the C(4)=O(4) distance (Table 2), apparently because only the O(2) atom participates in the hydrogen bonding network whereas the O(4) atom remains free

Table 3Hydrogen bonds geometry in 1-methylhydantoin (**L**¹) and [Ni(H₂O)₄(1-mhyd)₂] (**1**) [Å and °].

D–H...A	d(H...A)	d(D...A)	<(DHA)
(L¹)			
N(3)–H(3)...O(2)#1	1.888(19)	2.8148(17)	173.5(16)
C(1)–H(13)...O(4)#2	2.75(3)	3.450(2)	136(2)
C(5)–H(52)...O(2)#3	2.598(19)	3.455(2)	147.2(13)
Symmetry codes: #1 –x, –y, –z; #2 x + 1, –y + 1/2, z + 1/2; #3 –x + 1, y + 1/2, –z + 1/2			
(1)			
OW1–H(1W1)...O(2) #1	1.88	2.673(2)	146.7
OW1–H(2W1)...O(4)	1.86	2.658(2)	156.8
OW2–H(1W2)...O(4)#2	1.93	2.803(2)	178.6
OW2–H(2W2)...O(2)#3	1.97	2.794(2)	172.7

Symmetry codes: #1 –x, –y + 1, –z + 1; #2 –x, y + 1/2, –z + 3/2; #3 –x + 1, –y + 1, –z + 1.

(Fig. 1b, Table 3). The most prominent pattern of hydrogen bonds is the centrosymmetric ring $R_2^2(8)$ formed by the classic N–H...O interactions. The O(2) atom takes part also in the C–H...O interaction. This non-conventional hydrogen bonding connects 1-methylhydantoin molecules together resulting in a binary chain pattern, $C_2^2(10)$ (Fig. 1b). Other binary chain patterns can be also distinguished. However, neither of them describes the large ring, $R_6^4(22)$. All of the rings and chains are part of undulated pattern of hydrogen bonding parallel to the (–1 0 2) plane. Since the N(3)–H(3)...O(2) interaction (not shown in Fig. 1) is in plane of the 1-methylhydantoin molecule, the undulation is associated with the weak non-conventional C(5)–H(52)...O(2) moiety and sp³ hybridisation of the C(5) atom.

Overall, the hydrogen bonding architecture of 1-methylhydantoin differs significantly from the 5,5-disubstituted analogues,

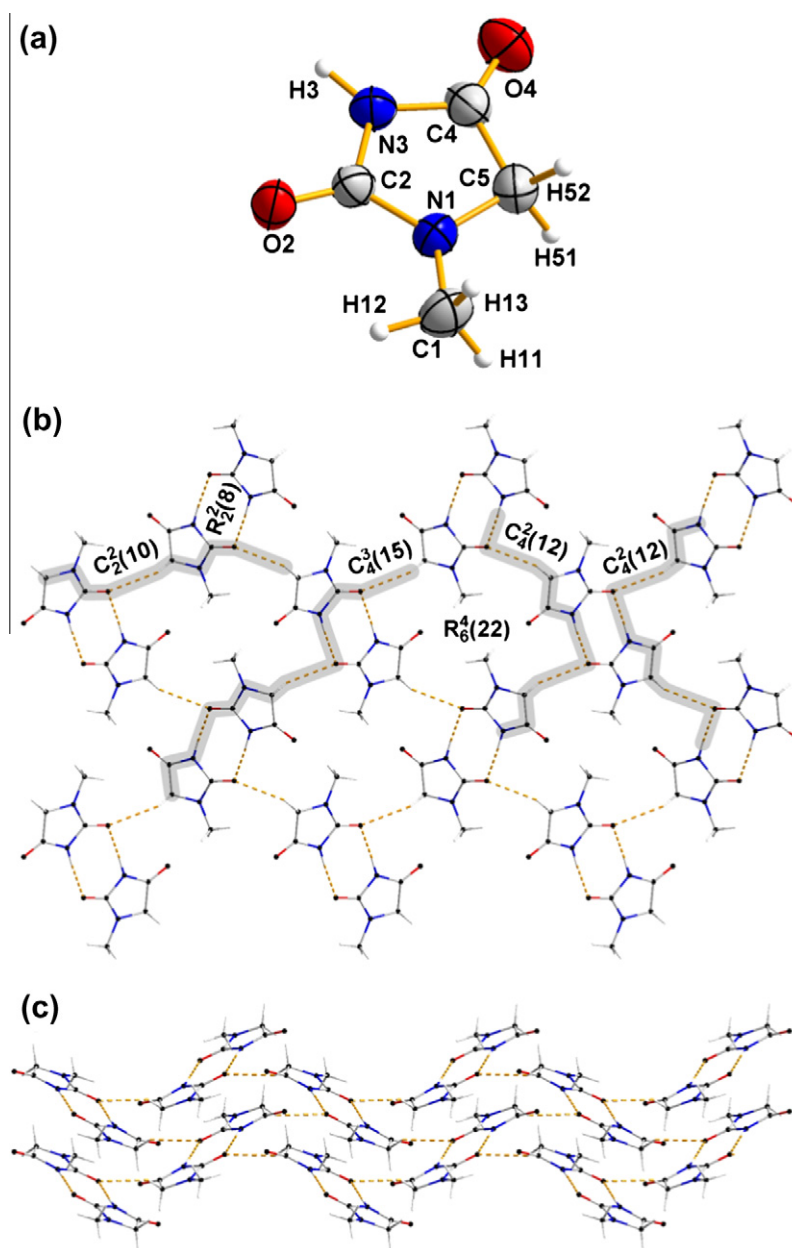


Fig. 1. (a) Atomic numbering scheme for 1-methylhydantoin. Displacement ellipsoids are drawn at the 50% probability level and H atoms are shown as small spheres of arbitrary radii. (b) Hydrogen bonding pattern parallel to the (–1 0 2) plane shows (c) undulated feature.

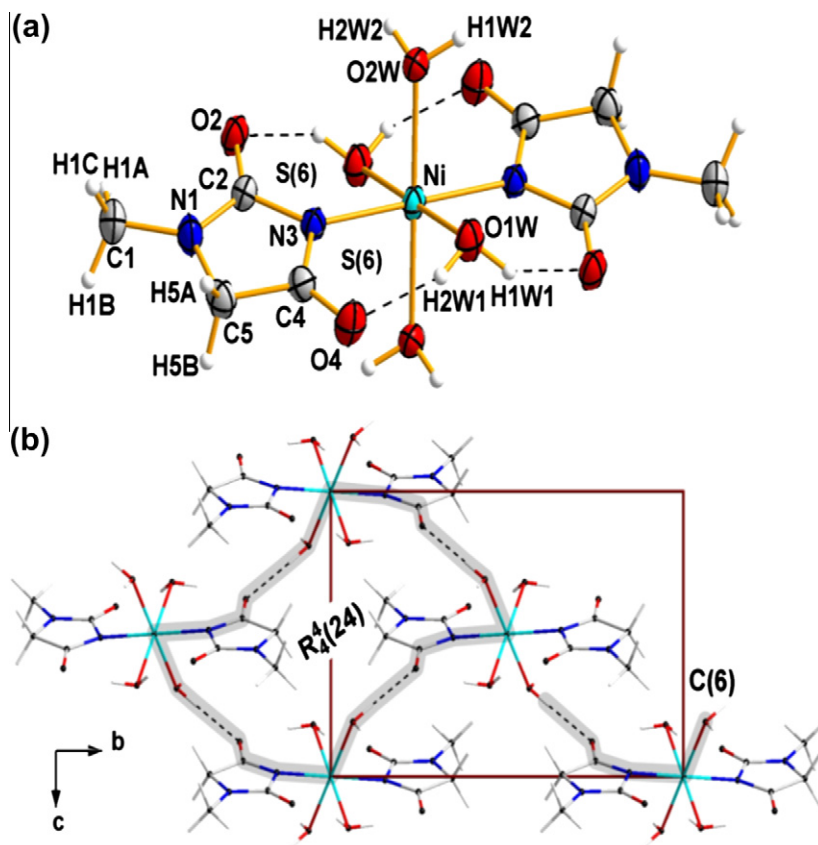


Fig. 2. (a) Molecular structure of $[\text{Ni}(\text{H}_2\text{O})_4(1\text{-mhyd})_2]$. (b) The chain and ring patterns constructed by $\text{O}2\text{W}-\text{H}1\text{W}2\cdots\text{O}4$ hydrogen bonds viewed along the a -axis.

Table 4
Selected IR bands for the 1-methylhydantoin and the complex: $[\text{Ni}(\text{H}_2\text{O})_4(\text{mhyd})_2]$ (**1**).

(L ¹)	(1)	Assignment [36,37]
3140w	–	$\nu(\text{N}(3)-\text{H})$
–	3368w	$\nu(\text{H}_2\text{O})$ for (1)
3045w 2955w	3086w 2810w	$\nu(\text{C}-\text{H})$
1768m	1723w	$\nu(\text{C}=\text{O})$
1709m	1666s	$\nu(\text{C}=\text{O})$
–	1609s	$\delta(\text{H}_2\text{O})$ for (1)
1592w	–	$\delta(\text{C}-\text{N}-\text{H})$
1499s	1479m	$\delta(\text{C}-\text{N}-\text{H})$
1414s	–	$\delta(\text{N}-\text{H})$
1374w	1396s	–
1350m	–	$\nu(\text{C}-\text{N})$
–	1300m	–
–	806m	$\rho(\text{H}_2\text{O})$
–	442s	$\nu(\text{M}-\text{O})$
–	324s	$\nu(\text{M}-\text{N})$

Abbreviations: vs, very strong; s, strong; m, medium; w, weak; vw, very weak.

because the N1 atom cannot participate in hydrogen bonding network as a donor of proton.

3.2. Crystal structure of $[\text{Ni}(\text{H}_2\text{O})_4(1\text{-mhyd})_2]$ (**1**)

Complex (**1**) crystallizes in a centrosymmetric space group (Table 1) with the nickel(II) ion positioned on the inversion centre. The asymmetric unit contains one 1-methylhydantoin anion and two water molecules. The six coordination sphere of the nickel(II) ion is completed by two additional water molecules and 1-mhyd anion generated by the inversion (Fig. 2).

Thus, the ligands create tetragonal coordination sphere around the metal centre with the 1-mhyd anions arranged in a *trans* position. The Ni–N and Ni–OW1 bond lengths are shorter than Ni–OW2 distances (Table 2) and they are similar to those found in the previously reported $[\text{Ni}(\text{NH}_3)_2(\text{H}_2\text{O})_2(\text{pht})_2]$ and $[\text{Ni}(\text{H}_2\text{O})_4(\text{pht})_2]$ (pht = 5,5-diphenylhydantoin) [34,35]. The real point group symmetry of the $[\text{Ni}(\text{H}_2\text{O})_4(\text{mhyd})_2]$ molecule is C_i . However, the corresponding interatomic angles within the coordination sphere differ insignificantly from the ideal octahedral values and the geometric parameters of the *trans*- $[\text{NiN}_2\text{O}_4]$ chromophore correlate with the D_{4h} point group symmetry.

The water molecule, OW1, forms two intramolecular hydrogen bonds (Table 3), both denoted by the S(6) graph set (Fig. 2a). Since the two OW1 water molecules which are present in the coordination sphere of the nickel(II) ion are related to each other by the inversion centre, four intramolecular hydrogen bonds are created in one molecule of $[\text{Ni}(\text{H}_2\text{O})_4(\text{mhyd})_2]$ (Fig. 2). The second independent water molecule OW2, participates in the inter-molecular hydrogen bonding networks. It is noteworthy, that one $\text{O}2\text{W}-\text{H}1\text{W}2\cdots\text{O}4$ hydrogen bond creates a unitary chain pattern, C(6), and it also forms separately a large ring pattern, $R_4^1(24)$, (Fig. 2b).

Overall, the complexes $[\text{Ni}(\text{H}_2\text{O})_4(1\text{-mhyd})_2]$ (**1**) and $[\text{Ni}(\text{H}_2\text{O})_4(\text{pht})_2]$ [35] have equivalent compositions and similar structures. However, they exhibit a different arrangement of HB networks. For example, in the former, the N1 atom, being methylated, cannot form hydrogen bonds.

3.3. Infrared spectra

Table 4 presents the most important IR vibrations for both the ligand and (**1**), together with proposed assignments. In the IR spectrum of $[\text{Ni}(\text{H}_2\text{O})_4(\text{mhyd})_2]$ (**1**) one may expect some new bands

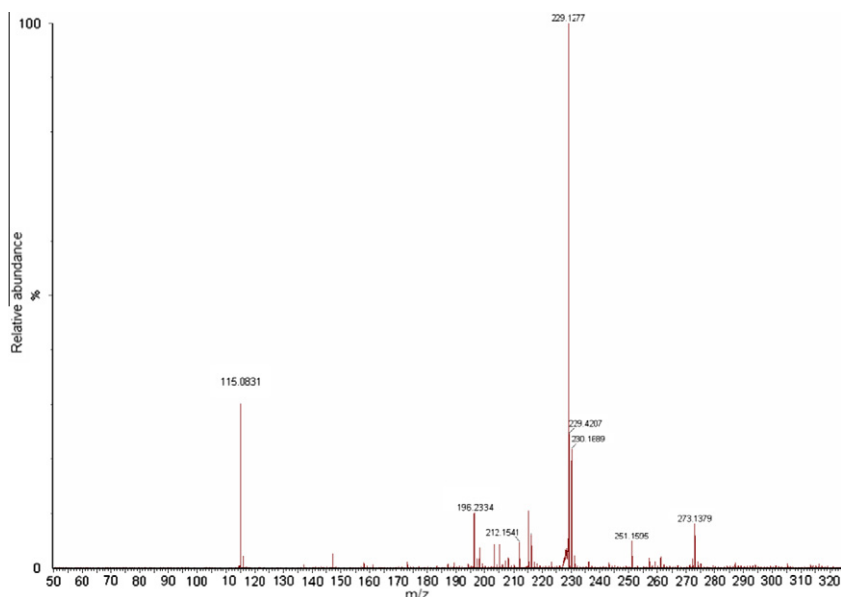


Fig. 3. Mass spectrum (ESI-MS) for 1-mhyd (L^1) in methanol.

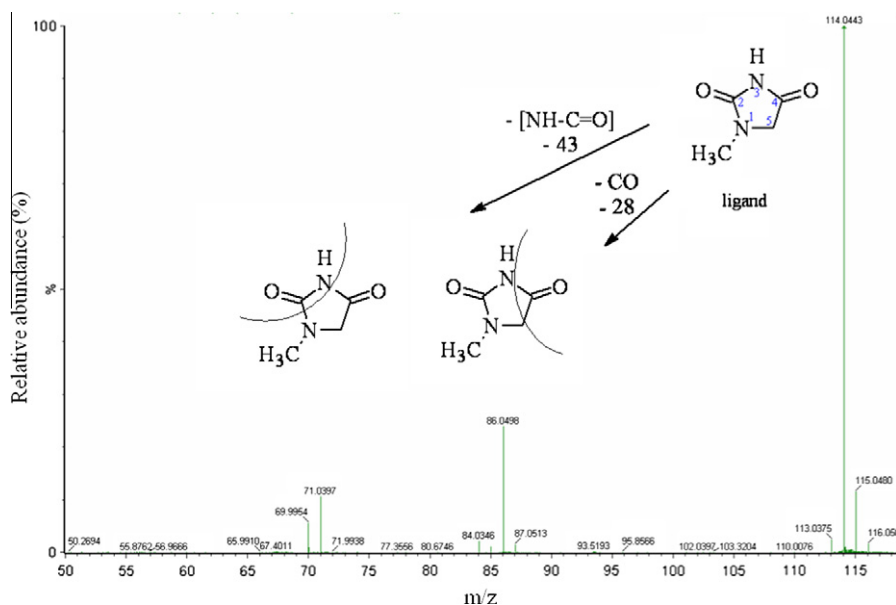


Fig. 4. Mass spectrum (EI) and fragmentation scheme for 1-mhyd (L^1).

appearing due to M–L vibrations and some changes in the organic ligand, e.g. disappearance of the N(3)–H(3) vibrations. In addition, the bathochromic shift of the $\nu_{C=O}$ vibrations due to formation of the HB between CO and H_2O molecules can be expected (Fig. 2a). As IR spectra of solid 1-mhyd are not available, the interpretation was made on the basis of its known solution spectra and spectrum of the parent hydantoin [36,37].

The comparative analysis of the IR spectra of 1-mhyd and its Ni(II) complex confirmed the expected bathochromic shift of $\nu_{(C4=O(4))}$ and $\nu_{(C2=O(2))}$ vibrations in (**1**) (Table 4), equal to ca. 40 cm^{-1} . The change of the band positions and their intensities in (**1**) is related mainly to the hydrogen bond formation involving carbonyl oxygen atoms and OW1 and OW2 of coordinated water molecules (Fig. 2a). The bands at 3368 cm^{-1} and 806 cm^{-1} in the spectrum of (**1**), were assigned to the stretching $\nu(H_2O)$ and rocking $\rho(H_2O)$ vibrations of water, respectively.

In FTIR spectra of the complex new bands at 324 cm^{-1} and 442 cm^{-1} were assigned to $\nu(M-N)$ and $\nu(M-O)$ stretching vibrations, respectively [38,39].

3.4. Mass spectrometry

Two spectrometric techniques were used to characterize the ligand: ESI-MS and EI. The first one is used for molecular mass determination while the second one to show the fragmentation pattern.

The ESI-MS spectrum of (L^1) (Fig. 3) shows a molecular peak at m/z 115.0625, which can be assigned to the protonated ligand [$(L^1)H$] $^+$. Additionally, the presence of ligand dimer has been also detected (Fig. 3).

1-mhyd decomposes during the EI processes producing various ions, among them two of significant intensity: at m/z 86.0498 and 71.0397 (Fig. 4). These particular forms are attributed to the loss of

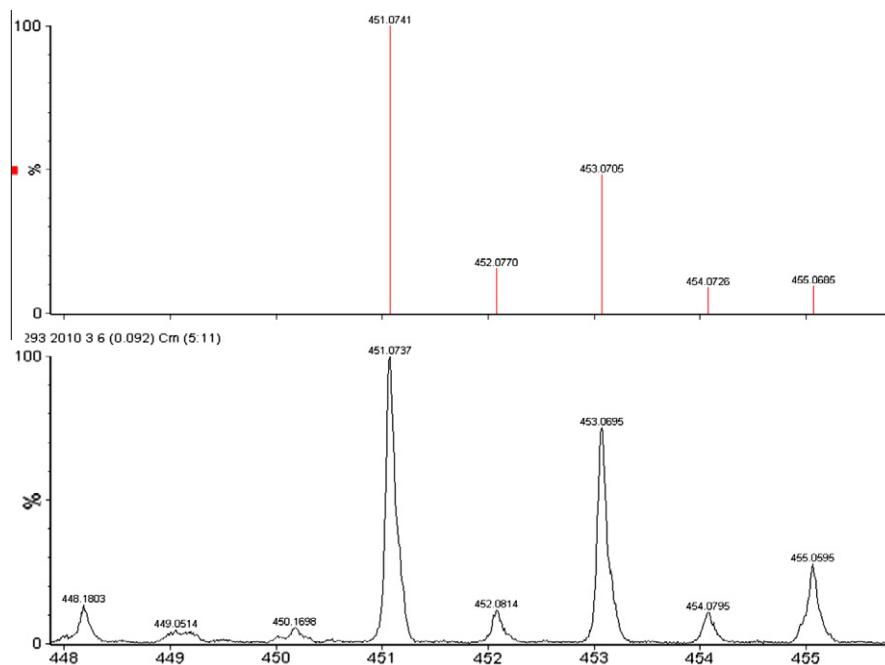


Fig. 5. ESI-MS spectra of complex (**1**) in methanol. Theoretically calculated isotope (top) and experimental (bottom) patterns of peaks with m/z 451.0737 assigned as $[\text{Ni}(\text{CH}_3\text{OH})_4(1\text{-mhyd})_2 + \text{K}]^+$.

CO ($-28u$) and/or NHCO ($-43u$), both fragments of 1-mhyd. This mode of decomposition was observed also for other hydantoin derivatives [40,41]. Carbon monoxide originates from C(4)=O(4) fragments earlier identified with isotopic labelling techniques [42]. The pathway of fragmentation indicates that the CH_3 substituent remains in the final residue upon ligand decomposition. Furthermore, it supports the earlier findings of poor stability of hydantoin [40].

The molecular formula of complex (**1**) was corroborated by signals at m/z 451.0737 assigned to $[\text{Ni}(\text{CH}_3\text{OH})_4(1\text{-mhyd})_2 + \text{K}]^+$ (see Fig. 5 and Section 2). The presence of methanol molecules in the observed peak results from substitution of water with this solvent during dissolution of the complex. For verification, complex (**1**) was additionally dissolved in acetonitrile but this did not show the solvent effect. Fig. 5 shows a comparison of the theoretically calculated nickel isotope envelope of peaks with the experimental results.

3.5. Electronic spectra of complex (**1**)

The crystallographic data revealed that microsymmetry of the nickel surroundings in complex (**1**) is tetragonal (D_{4h}). The splitting of the first d–d band in the reflectance spectra is in line with this approach (Fig. 6a). However, in solution, the bands exhibit only some asymmetry (Fig. 6b) thus for this phase the analysis assuming pseudo-octahedral approximation has been carried out. Additionally, the value of the ϵ coefficient (6.5) is in line with the respective values for $[\text{Ni}(\text{A}_2\text{B}_4)]$ [27,59]. In the literature both approaches i.e. pseudo-octahedral and tetragonal were used in the interpretation of the $[\text{Ni}(\text{A}_2\text{B}_4)]$ complexes (see for example [59,60]). As there is no clear criterion we adopt here a distinct splitting of the d–d bands (at least one) in the spectrum as a condition for a tetragonality. The results are presented in Scheme 2, Table 5 and Fig. 6. For solution phase (pseudo-octahedral symmetry) the crystal field splitting (10Dq) and Racah B parameter (a measure of interelectronic repulsion) were obtained from the Tanabe–Sugano diagram (Table 5) [27]. In view of the fact that for D_{4h}

symmetry 10Dq has a slightly different meaning being *de facto* one of three parameters i.e. Dq, Ds, or Dt, describing the CF splitting (Table 5), the comparative analysis for O_h and D_{4h} symmetries was made taking into account only the Racah B parameter. Based on the data in Table 5, it can be concluded that for the pseudo-octahedral symmetry (solution) the B parameters are 48 cm^{-1} lower than those for D_{4h} . Thus, in the solid phase (D_{4h}), the ionicity of M–L bonds was higher than in solution. This may be a result of greater “individuality” of the species in the solution phase.

Generally, CF and Racah B values obtained here for the $[\text{NiNi}_2\text{O}_4]$ chromophore in (**1**) were found to be comparable to those for Ni(II) complexes reported previously [43].

As the 10Dq parameter is a measure of the ligand strength, it is also of interest to rank 1-methylhydantoin in the spectrochemical series of ligands [27]. By application of the “average environment rule” [44] i.e. based on the expression $\Delta[\text{Ni}(\text{H}_2\text{O})_4\text{L}_2] = 1/6 \{4\Delta[\text{Ni}(\text{H}_2\text{O})_6]^{2+} + 2\Delta[\text{NiL}_6]^{4-}\}$ the values for 10Dq for hypothetical $[\text{Ni}(1\text{-mhyd})_6]^{4-}$ (assuming a monodentate coordination) can be estimated and it was found to be equal to 10750 cm^{-1} . (The Δ values for $[\text{Ni}(\text{H}_2\text{O})_4\text{L}_2]$ and $[\text{Ni}(\text{H}_2\text{O})_6]^{2+}$ are 9250 cm^{-1} (this work) and 8500 cm^{-1} [27], respectively). As a matter of fact, due to the size of the ligand and its more than one donor atoms, a more realistic formula for the compound should be $[\text{Ni}(1\text{-mhyd})_3]^-$ chelate.

Thus, 1-methylhydantoin can be placed in the spectrochemical series for the octahedral NiL_6 (and pseudo-octahedral $\text{Ni}(\text{L-L})_3$) complexes with one type of ligand as follows (the magnitudes of splitting in cm^{-1} given in brackets):

H_2O (8500) < py (10 150) < NH_3 (10 750) < 1-mhyd (10 750) < en (11 700) < bpy (12 650).

The position of 1-mhyd close to ammonia suggests that the average environment rule can be applicable to this complex. Thus, on the spectrochemical scale the 1-mhyd was found to be a rather moderately strong one.

The value of the experimental magnetic moment obtained for the nickel(II) complex is $2.77\ \mu_B$ (see Section 2). This value is slightly lower than those usually observed for nickel(II) octahedral complexes (μ_{eff} 2.90, μ_{so} 2.83 μ_B) [45–47]. The lowering of μ value

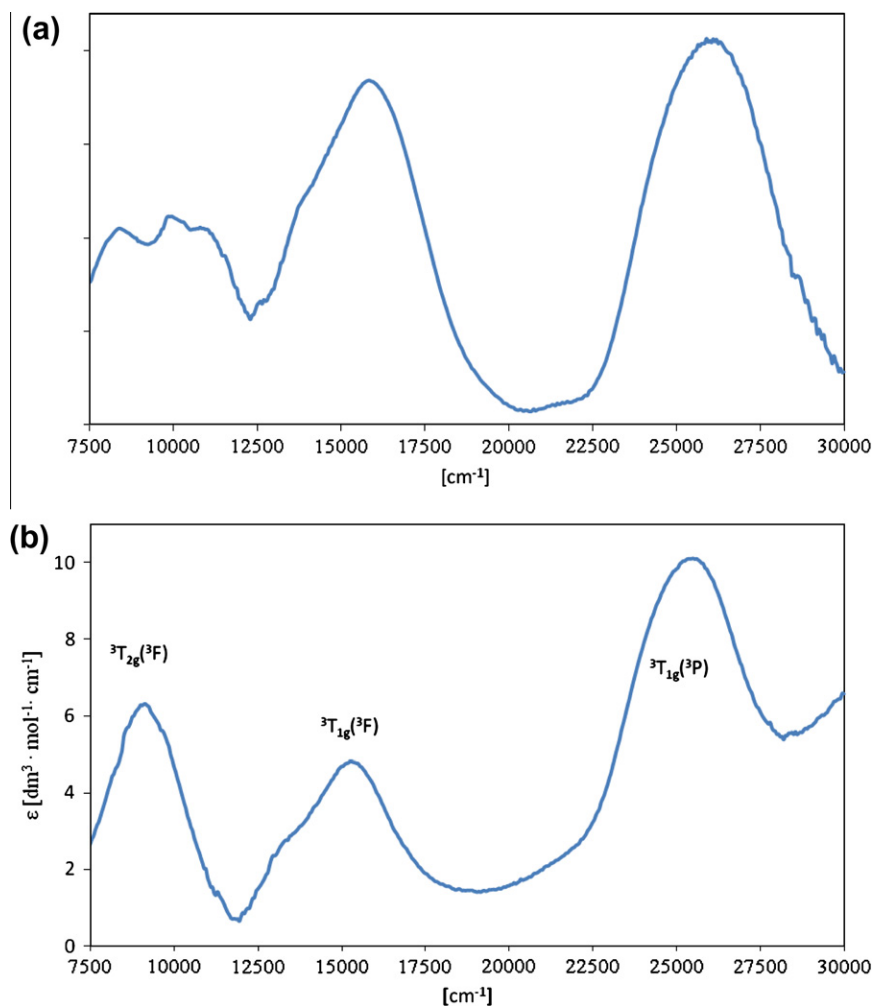


Fig. 6. Spectrum of $[\text{Ni}(\text{H}_2\text{O})_4(1\text{-mhyd})_2]$ in the solid phase (a) and methanol (b).

can be attributed to the real symmetry of (**1**) which is lower than O_h [27].

3.6. Thermal decomposition

The main goal of thermogravimetric studies was to confirm (indirectly) the presence and position of water molecules in the complex (**1**). Generally, the loss of coordinated water is manifested through endothermic effect in the range between 140 and 230 °C while the water of crystallization is released earlier i.e., between 50 and 120 °C [48,49]. TG and DTA data for the complex (**1**) showed the weight loss between 140 and 220 °C, which is attributable to the elimination of four water molecules from the first coordination sphere (mass loss 20.17%, 22.74%, calculated and found, respectively). This observation is supported by the enthalpy changes (endothermic effect – 32 kJ/mol) related to the complete loss of coordination water in (**1**). The observed weight loss during the next step is in accordance with the calculated value for the release of two hydantoin molecules (55.13% and 58.86% calculated and found, respectively). The subsequent decomposition occurs between 220 and about 600 °C, leading finally to NiO (exp. solid residue 22.13 calcd. 20.90%).

Summing up, the results of analysis, IR and solid state electronic spectra, mass spectroscopy and thermal data are consistent with the structure determined by X-ray analysis for (**1**).

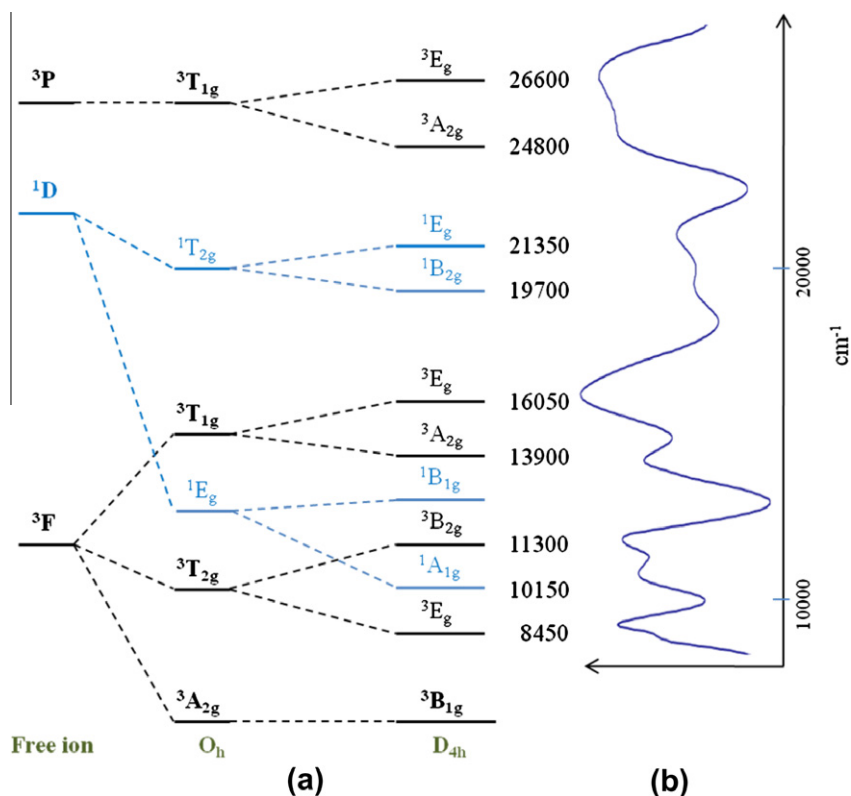
3.7. Complexes of hydantoins with “soft”, “borderline” and “hard” Lewis acids

The literature search showed that 1-methylhydantoin complex with Ni(II) (**1**) is the first isolated species of this ligand with the borderline metal cation (HSAB). The others examples are very soft (Au^+) and soft (Pt^{2+} , Ag^+ , Hg^{2+}) (Table 6).

Analysis of the binding modes of metal ion complexes with other hydantoins (Table 6) provides some general observations on the structure of their first coordination spheres in relation to the metal ionic radius and its hardness. The following relationships have been observed:

- For a very soft (Au^+) and a very hard (K^+) cations (both are very large, see Table 6) the coordination of hydantoins is monodentate through N and O atoms, respectively.
- The same mode of coordination is valid for small borderline cations (Ni^{2+} and Zn^{2+}) but exclusively through N atoms.
- Soft cations but smaller than Au^+ can coordinate through N to one metal ion and O to the other forming a coordination polymer.

It can be stated that the HSAB principle is valid for hydantoin complexes as a very soft Au^+ does not interact with oxygen, whereas soft Lewis acids have preference for both donors, consequently forming polynuclear forms [57]. On the contrary, a very



Scheme 2. Correlation diagram (d^8 configuration) for O_h and D_{4h} symmetries (a) and the effect of filtration of the solid state spectrum of (1) (b).

Table 5

The band positions, assignment of the electronic spin-allowed transitions in the spectra and crystal field and Racah B parameters for $[Ni(H_2O)_4(mhyd)_2]$ (1) (in cm^{-1}).

Absorption		Reflectance	
<i>Transition from ground state (${}^3A_{2g}$)</i>			
O_h		D_{4h}^a	
${}^3T_{2g}$ (3F)	9000	3E_g	8450
		${}^3B_{2g}$	11300
${}^3T_{1g}$ (3F)	15100	${}^3A_{2g}$	13900
		${}^3E_{2g}$	16050
${}^3T_{1g}$ (3P)	25300	${}^3A_{2g}$	24800
		3E_g	26600
<i>CF and Racah parameters</i>			
Dq	925	D_{4h}^a	
B	841	1148	
$-Dt$	-	889	
Ds	-	329	
		172	

^a Resolved with the digital filtration.

hard cation (K^+) shows, as expected, preference for the oxygen atom of the ligand.

The borderline small cations (Zn^{2+} , Ni^{2+}) bind to nitrogen atom of the ligand with formation of mononuclear complexes.

As the above observations are based on limited data, more studies are needed to verify the information included in Table 6.

3.8. Antiproliferative activity

The compounds 1-mhyd (L^1) and its Ni(II) complex (1) were subjected to cytotoxic activity tests carried out *in vitro* against three cancer cell lines: breast (MCF-7), lung (A549) and mouse cell line fibroblasts mouse fibroblast cell line (Balb/3T3). The results revealed that in the studied concentration range both the ligand and

its nickel complex are inactive in the inhibition of cell proliferation. In general, hydantoin are found to be cytotoxically inactive but the complexation to a metal ion e.g. Ag^+ may produce strong proliferative agents [14,58]. This activity was found to be also a cell line selective [58]. The present work shows no cytotoxic activity of both the ligand and its Ni complex.

4. Summary and conclusions

1-Methylhydantoin interacts with Ni(II) ion to form a mononuclear mixed ligand species of the formula *trans*- $[Ni(H_2O)_4L_2]$. The single crystal X-ray diffraction data revealed an interesting HB network both in the free ligand (classic and non-conventional) and in the complex (conventional intramolecular bonding). The analysis of electronic spectra showed the significance of the phase and the adopted symmetry model in the calculation of the crystal field parameters. In the spectrochemical series 1-methylhydantoin was found to be positioned close to ammonia, i.e. appearing as a moderately ligand. Both 1-methylhydantoin and its nickel complex exhibited no cytotoxic activity *in vitro* against three cancer cell lines.

Comparative analysis of the mixed ligand Ni(II) complex with 1-methylhydantoin and other hydantoin derivative complexes shows dependence of the mode of ligand binding upon metal ion hardness in the frame of the HSAB theory. Both very soft and very hard Lewis acids coordinate this ligand through only one donor atom: nitrogen and oxygen, respectively. With soft acids polynuclear species were formed due to binding through N(3) donor atom to one metal central atom and oxygen atom to the other. For borderline Lewis acids the coordination is mononuclear again. The results of the current work combined with the literature data can be used as the basis for further studies on the structural dependence of hydantoin complexes upon metal hardness.

Table 6

The mode of ligand coordination in hydantoin derivatives in relation to metal hardness [50,51] and ionic radius [52].

Metal ion		Hardness (η)	Ionic radius (pm)	Donor atoms coordinated to the metal ions			References
				1-Methylhydantoin	5,5-Diphenylhydantoin	5,5-Dimethylhydantoin	
Soft	Au ⁺	5.4	137	N(3)	–	–	[11]
	Ag ⁺	6.9	115	N(3), O(4)	–	–	[14]
	Hg ²⁺	7.7	102	N(3), O(4)	–	–	[13]
	Pt ²⁺	8.0	86	N(3), O(4)	–	–	[12]
Border line	Cu ²⁺	8.3	73	–	N(3)	–	[53]
	Au ³⁺	8.4	85	–	–	N(3)	[54]
	Ni ²⁺	8.5	69	N(3) (this work)	N(3)	–	[34]
	Zn ²⁺	10.8	75	–	N(3)	–	[55]
Hard	K ⁺	13.6	138	–	O(4)	–	[56]

Acknowledgments

The authors are thankful to Ms. E. Mróz and Dr. A. Adach for their help in recording of IR spectra and thermal decomposition analysis, respectively. The helpful comments and language correction from Dr. W. Roth are greatly acknowledged. The author (MPT) wishes to acknowledge the Polish Ministry of Higher Education and Science for financial support (grant no. NN204 331037). Grant from Wrocław University of Technology is also acknowledged.

Appendix A. Supplementary material

CCDC 784164 and 784168 contains the supplementary crystallographic data for ligand (**L**¹) and compound (**1**). These data can be obtained free of charge via <http://www.ccdc.cam.ac.uk/conts/retrieving.html>, or from the Cambridge Crystallographic Data Centre, 12 Union Road, Cambridge CB2 1EZ, UK; fax: (+44) 1223-336-033; or e-mail: deposit@ccdc.cam.ac.uk.

References

- [1] S.S. Block, *Disinfection, Sterilization and Preservation*, fourth ed., Lea & Febiger, Philadelphia, 2003.
- [2] C.S.A. Kumar, S.B.B. Prasad, K. Vinaya, S. Chandrappa, N.R. Thimmegowda, S.R. Ranganatha, S. Swarup, K.S. Rangappa, *Invest New Drugs* 27 (2009) 131.
- [3] C.V. Kavitha, M. Nambiar, C.S. Ananda Kumar, B. Choudhary, K. Muniyappa, K.S. Rangappa, S.C. Raghavan, *Biochem. Pharmacol.* 77 (2009) 348.
- [4] R. Sarges, R.C. Schnur, J.L. Belletire, M.J. Peterson, *J. Med. Chem.* 31 (1988) 230.
- [5] A.J. van Dam, *Coll. Forum* 18 (2003) 104.
- [6] R. Vardanyan, H.J. Hruby, *Synthesis of Essential Drugs*, Elsevier, 2006.
- [7] K. Yang, Y. Tang, K.A. Iczkowski, *Am. J. Trans. Res.* 2 (2010) 88.
- [8] H.-S. Park, H.-J. Choi, H.-S. Shin, S.K. Lee, M.-S. Park, *Bull. Korean Chem. Soc.* 28 (2007) 751.
- [9] *Cosmetic Safety Database*.
- [10] G. Maciejewska, W. Zierkiewicz, A. Adach, M. Kopacz, I. Zapała, I. Bulik, M. Cieślak-Golonka, T. Grabowski, J. Wietrzyk, *J. Inorg. Biochem.* 103 (2009) 1189.
- [11] N.A. Malik, P.J. Sadler, S. Neidle, G.L. Taylor, *J.C.S. Chem. Commun.* 625 (1978) 711.
- [12] J.P. Laurent, P. Lepage, F. Dahan, *J. Am. Chem. Soc.* 104 (1982) 7335.
- [13] D.M.L. Goodgame, A.M. Khaled, C.A. O'Mahoney, D.J. Williams, *Polyhedron* 9 (1990) 1765.
- [14] M. Puszyńska-Tuszkano, T. Grabowski, M. Daszkiewicz, J. Wietrzyk, B. Filip, G. Maciejewska, M. Cieślak-Golonka, *J. Inorg. Biochem.* 105 (2011) 17.
- [15] R.G. Pearson, J. Songstad, *J. Am. Chem. Soc.* 89 (1967) 1827.
- [16] R.G. Pearson, *J. Am. Chem. Soc.* 85 (1963) 3533.
- [17] R. Śpiewak, J. Pietowska, K. Curzytek, *Expert Rev. Clin. Immunol.* 3 (2007) 851.
- [18] G. Bierman, H. Ziegler, *Anal. Chem.* 58 (1986) 536.
- [19] J. Myrczek, *Spectrosc. Lett.* 23 (1990) 1027.
- [20] M. Cieślak-Golonka, M. Raczko, Z. Staszak, *Polyhedron* 11 (1992) 2549.
- [21] A. Wojciechowska, Z. Staszak, A. Pietraszko, W. Bronowska, M. Cieślak-Golonka, *Polyhedron* 21 (2001) 2063.
- [22] A. Pietraszko, *Pol. J. Chem.* 76 (2002) 309.
- [23] A. Bardecki, Z. Staszak, *Comp. Enh. Spectrosc.* 2 (1984) 129.
- [24] D. Miernik, A. Arkowska, E. Gzrzyńska, Z. Staszak, *Spectrosc. Lett.* 24 (1991) 371.
- [25] J.R. Perumareddi, *J. Phys. Chem.* 76 (1972) 3401.
- [26] J.S. Merriam, J.R. Perumareddi, *J. Phys. Chem.* 79 (1975) 142.
- [27] A.B.P. Lever, *Inorganic Electronic Spectroscopy*, second ed., Elsevier, New York, 1984.
- [28] G.M. Sheldrick, *Acta Crystallogr., Sect. A* 64 (2008) 112.
- [29] R.I. Geran, N.H. Greenberg, M.M. MacDonald, A.M. Schumacher, B.D. Abbott, *Cancer Chemother. Rep.* 3 (1972) 59.
- [30] F.-L. Yu, C.H. Schwalbe, D.J. Watkin, *Acta Crystallogr., Sect. C* 60 (2004) o714.
- [31] D. Mootz, *Acta Cryst.* 19 (1965) 726.
- [32] T.K. Chattopadhyay, R.A. Palmer, J.N. Lisgarten, *J. Crystallogr. Spectrosc. Res.* 23 (1993) 149.
- [33] R.E. Cassidy, S.W. Hawkinson, *Acta Crystallogr., Sect. B* 38 (1982) 1646.
- [34] N. Shimizu, T. Uno, *Cryst. Struct. Commun.* 9 (1980) 389.
- [35] M. Puszyńska-Tuszkano, M. Daszkiewicz, G. Maciejewska, A. Adach, M. Cieślak-Golonka, *Struct. Chem.* 21 (2010) 315.
- [36] Y. Saito, K. Machida, *Bull. Chem. Soc. Jpn.* 51 (1987) 108.
- [37] T. Kimura, Y. Nagao, *Bull. Fac. Sci. Tech. Hirosaki Univ.* 5 (2003) 11.
- [38] K. Kurdziel, T. Głowiak, *Polyhedron* 19 (2000) 2183.
- [39] J. Titis, R. Boca, L. Dihan, T. Durcekova, H. Fuess, R. Ivanicova, V. Mrazova, B. Papankova, I. Svoboda, *Polyhedron* 26 (2007) 1523.
- [40] J.X. Shen, J. Brodbelt, *J. Mass Spectrom.* 31 (1996) 1389.
- [41] S. Schöhl, I. Bloß, W. Rudiger, *Org. Mass Spectrom.* 10 (1975) 798.
- [42] E. Kleinpeter, *Struct. Chem.* 8 (1997) 161.
- [43] W. Bronowska, Z. Staszak, M. Daszkiewicz, M. Cieślak-Golonka, A. Wojciechowska, *Polyhedron* 21 (2002) 997.
- [44] A.B.P. Lever, S.M. Nelson, T.M. Shepherd, *Inorg. Chem.* 4 (1965) 810.
- [45] S. Chandra, R. Kumara, R. Singh, *Spectrochim. Acta A* 65 (2006) 215.
- [46] R.K. Agarwal, D. Sharma, L. Singh, H. Agarwal, *Bioinorg. Chem. Appl.* 1 (2006) 1.
- [47] Y. Inomata, M. Ando, F.S. Howell, *J. Mol. Struct.* 616 (2002) 201.
- [48] E. Ingier-Stocka, M. Maciejewski, *Thermochim. Acta* 432 (2005) 56.
- [49] F. Paulik, *Spectral Trends in Thermal Analysis*, Wiley, 1995.
- [50] R.B. Martin, *Inorg. Chim. Acta* 283 (1998) 30.
- [51] R.G. Peterson, *Inorg. Chem.* 27 (1988) 734.
- [52] R.D. Shannon, *Acta Crystallogr., Sect. A* 32 (1976) 751.
- [53] X.-L. Hu, X.-Y. Xu, D.-Q. Wang, T.-T. Xu, *Acta Crystallogr., Sect. E* 62 (2006) m1922.
- [54] K. Oyaizu, Y. Ohtani, A. Shiozawa, K. Sugawara, T. Saito, M. Yuasa, *Inorg. Chem. Commun.* 44 (2005) 6915.
- [55] A.W. Roszak, P. Milne, *Acta Crystallogr., Sect. C* 51 (1995) 1297.
- [56] P.S. Pereira Silva, M. Ramos Silva, J.A. Paixao, A. Matos Beja, *J. Chem. Crystallogr.* 36 (2009) 669.
- [57] M. Goodgame, D.A. Jacobovic, *Coord. Chem. Rev.* 79 (1987) 97.
- [58] B. Yang, D. Liu, C.Z. Li, F.Y. Liu, Y.M. Peng, Y.S. Jiang, *Ren. Fail.* 29 (2007) 1025.
- [59] D.J. Radanovic, V.C. Matovic, Z.D. Matovic, L.P. Battaglia, G. Pelizzi, G. Ponticelli, *Inorg. Chim. Acta* 237 (1995) 151.
- [60] S. Kammoun, M. Dammak, R. Maalej, M. Kamoun, *J. Lumin.* 124 (2007) 316.